exposure to reduced pressure. Also in contrast to the case for the other complexes, the CN stretch ($\nu_{CN}$ = 2252 cm$^{-1}$) does not decrease in intensity even after repated cycling. In the presence of air, the ability of [P]-$CH_2Cl$·CuCl·$n$$CH_3CN$ to bind CO is drastically reduced and an ESR signal is observed. This complex is apparently not present in significant concentrations in [P]-(DCEA)CuX and [P]-$N(CH_3)_2$CuX. In the case of [P]-$N(CH_3)_2$CuX a large change in $\nu_{CO}$ is observed and no CN stretch is observed. Although the $\nu_{CO}$ frequencies of [P]-$CH_2Cl$ and [P]-DCEA adducts of CO are similar, the [P]-(DCEA)CuX complex must be pumped on to remove solvating $CH_3CN$ before CO complexation occurs, whereas [P]-$CH_2Cl$·CuCl·$n$$CH_3CN$ binds CO without such pretreatment.

In conclusion, heterogenizing copper(I) halides on functionalized cross-linked polystyrene has afforded both complexes and reactivity not observed in solution. As demonstrated above, the polymer matrix serves to provide a hydrophobic environment that appears to stabilize Cu(I) salts in the solid state. One of the advantages of the polymer-supported complexes is the elimination of lattice energy effects present in many solid-state metal complexes, which prevent small-molecule binding. The permeability and functional groups in the polymer provide variables permitting one to adjust the extent and rates of carbonylation. We expect these supported Cu(I) complexes to find application in pressure-swing recovery or in the facilitated transport of CO in polymer membranes. Efforts in this regard are under way.

**Acknowledgment.** This research was supported by the National Science Foundation through Grant 86 18761.

**Registry No.** CuCl, 7758-89-6.

---

Contribution from The Institute of Physical and Chemical Research, Wako-shi, Saitama 351, Japan, and Dalian Institute of Chemical Physics, Academia Sinica, Dalian, China

# Preparation and Structural-Bonding Characterization of a 50-Electron Triangular Cobalt Cluster, $[Co(C_5H_4CO_2Me)]_3(S)(N^tBu)$, with Triply Bridging Sulfido and Imido Ligands: Singlet–Triplet Equilibrium in Solid and Solution States

Yasuo Wakatsuki,*[†] Takuya Okada,[†] Hiroshi Yamazaki,[†] and Guobao Cheng[‡]

*Received January 28, 1988*

A 50-electron tricobalt cluster, $[Co(C_5H_4CO_2Me)]_3(S)(N^tBu)$ (**1**), has been prepared by the reaction of $Co(C_5H_4CO_2Me)$(1,5-cyclooctadiene) with bis(*tert*-butylimido)sulfur. A magnetic susceptibility study carried out over a temperature range of 18–294 K revealed that in the solid state **1** has a singlet ground state with a triplet excited state ca. 0.3 kcal/mol above it. The solid-state molecular structure of **1** has been determined at room temperature from a single-crystal X-ray diffraction analysis. This molecule, which possesses a triangular metal framework with capping sulfido and *tert*-butylimido ligands, has no crystallographically imposed symmetry as is expected by the presence of noncylindrical monosubstituted cyclopentadienyl ligands. The metal triangle is significantly deformed from an equilateral configuration by crystal packing forces to give Co–Co bond lengths of 2.537 (1), 2.587 (1), and 2.610 (1) Å. The mean Co–Co bond length in **1** is ca. 0.13 Å longer than that of the known 48-electron $[CoCp]_3(S)(CO)$ cluster: this difference is attributed to the antibonding nature of the trimetal orbitals occupied by the two additional electrons in **1** in that both **1** and $[CoCp]_3(S)(CO)$ have ligands of similar size. Variable-temperature $^1H$ NMR data for **1** displayed paramagnetic isotropic shifts that were analyzed on the basis of a contact-shift equation in terms of a singlet–triplet equilibrium in solution. For comparison, $[Co(C_5H_4CO_2Me)]_3(S)_2$ (**2**) was prepared and likewise characterized from variable-temperature $^1H$ NMR measurements. A similar isotropic shift analysis revealed a contrasting singlet–triplet equilibrium for **2** in solution vs that for **1**. At 0 °C in solution, **1** has a triplet ground state with a singlet excited state ca. 0.8 kcal/mol higher in energy whereas **2** has a singlet ground state with a triplet-state energy level at ca. 0.7 kcal/mol higher position. It is suggested that the difference in these magnetic properties in solution originates from the size of the metal triangles, which controls the relative positions of an $a_2$ orbital and degenerate e orbitals. Complex **1**: triclinic, $P\bar{1}$, $a$ = 10.057 (3) Å, $b$ = 14.716 (4) Å, $c$ = 9.680 (3) Å, $\alpha$ = 92.15 (3)°, $\beta$ = 111.48 (2)°, $\gamma$ = 81.34 (3)°, $Z$ = 2, and $R$ = 0.046 for 4339 independent reflections.

## Introduction

Several electronically saturated (48 valence electrons) and diamagnetic tricobalt clusters have been reported; they have in common a 42-electron triangular $[CoCp]_3$, $[CoCp']_3$, or $[CoCp^*]_3$ fragment (where Cp = $\eta^5$-$C_5H_5$, Cp′ = $\eta^5$-$C_5H_4Me$, Cp* = $\eta^5$-$C_5Me_5$) containing electron-pair Co–Co bonds and a pair of capping ligands that donate 6 electrons: (CO)(O),[1] (CO)(S),[2,3] (CS)(S),[4] (CO)($NSiMe_3$),[5] (CO)($N(CO)NH_2$),[5] and (CO)(NH).[5] As for the 50-electron analogues, only two examples, $[CoCp]_3(\mu_3\text{-}S)_2$ (**3**)[6a] and $[CoCp']_3(\mu_3\text{-}S)_2$ (**3a**),[6b] have been reported. The two additional electrons in $[CoCp]_3(\mu_3\text{-}S)_2$ cause **3** to exist in a solid-state room-temperature phase with two unpaired electrons[2,6a] and in solution to possess a singlet–triplet equilibrium that shifts to the singlet state at lower temperatures.[6a] The corresponding methylcyclopentadienyl analogue was shown to be diamagnetic in the solid state (in accordance with its solid-state structure) but in solution to possess a singlet–triplet equilibrium that likewise shifts to the singlet state at lower temperatures.[6b] Recently, an interesting 46-electron analogue bicapped by two CO ligands, $[CoCp^*]_3(CO)_2$ (**4**), has been prepared and shown by Dahl and co-workers to possess a singlet–triplet equilibrium in solution similar to that of **3**.[7] In order to interpret the magnetic features of this class of compounds and thereby shed light on the spin and

[†] The Institute of Physical and Chemical Research.
[‡] Dalian Institute of Chemical Physics.

(1) Uchtman, V. A.; Dahl, L. F. *J. Am. Chem. Soc.* **1969**, *91*, 3763.
(2) Otsuka, S.; Nakamura, A.; Yoshida, T. *Liebigs Ann. Chem.* **1968**, *719*, 54.
(3) Otsuka, S.; Nakamura, A.; Yoshida, T. *Inorg. Chem.* **1968**, *7*, 261.
(4) Werner, H.; Leonhard, K.; Kolb, O.; Röttinger, E.; Vahrenkamp, H. *Chem. Ber.* **1980**, *113*, 1654.
(5) Bedard, R. L.; Rae, A. D.; Dahl, L. F. *J. Am. Chem. Soc.* **1986**, *108*, 5924.
(6) (a) Frisch, P. D.; Dahl, L. F. *J. Am. Chem. Soc.* **1972**, *94*, 5082. (b) Pulliam, C. R.; Englert, M. H.; Dahl, L. F. *Abstracts of Papers*, 190th National Meeting of the American Chemical Society, Chicago, Illinois; American Chemical Society: Washington, DC, 1985; INOR 387. See ref 7, pp 7654 and 7655, and footnote 45 in: Olson, W. L.; Dahl, L. F. *J. Am. Chem. Soc.* **1986**, *108*, 7657. (c) Kamijo, N.; Watanabe, T. *Acta Crystallogr., Sect B: Struct. Crystallogr. Cryst. Chem.* **1979**, *B35*, 2537.
(7) Olson, W. L.; Stacy, A. M.; Dahl, L. F. *J. Am. Chem. Soc.* **1986**, *108*, 7646.

0020-1669/88/1327-2958$01.50/0 

orbital states in cluster complexes, more examples have to be examined.

We report in this paper a new 50-electron paramagnetic tricobalt cluster having sulfido and imido capping ligands. This combination of S and $N(CMe_3)$ bridging ligands was not attainable by use of the conventional Cp ligand but instead by use of the methoxycarbonyl-substituted cyclopentadienyl ligand $C_5H_4CO_2Me$ (abbreviated as ZCp). The magnetic properties of this complex have been found to be different both in solution and in the solid state from those of **3** and **4**.

## Experimental Section

The starting complexes $Co(ZCp)(CO)_2$ and Co(ZCp)(cod) (cod = 1,5-cyclooctadiene) were prepared by known methods.[8,9] Proton NMR spectra were recorded on a JEOL GX-400 spectrometer in toluene-$d_8$ unless otherwise stated.

**Preparation of $[Co(ZCp)]_3(S)(N^tBu)$ (1).** A mixture of Co(ZCp)(cod) (585 mg, 2 mmol), benzene (20 mL), and $(^tBuN)_2S$ (450 mg, 2.64 mmol) was sealed in an ampule under nitrogen and heated at 120 °C for 20 h. The color changed from yellow to dark brown. After concentration the solution was chromatographed on an alumina column (deactivated beforehand with 10 wt % of water). A yellow band and a brown band separated. The first yellow band was eluted with benzene/hexane (1/1). After evaporation of the solvent, the residue was dissolved in a minimum amount of cold hexane to give yellow crystals of unreacted Co(ZCp)(cod) (144 mg). The second dark brown band was eluted with benzene/ethyl acetate (10/1), and the eluent was concentrated to ca. 2 mL. Addition of hexane gave dark crystals of **1** (100 mg; 44% yield based on consumed Co(ZCp)(cod)), mp 132–133 °C dec. Anal. Calcd for $C_{25}H_{30}Co_3NO_6S$: C, 46.2; H, 4.7; N, 2.2; S, 4.9. Found: C, 46.5; H, 4.6; N, 2.2; S, 4.9.

**Preparation of $[Co(ZCp)]_3(S)_2$ (2).** $Co(ZCp)(CO)_2$ (2.7 g, 11 mmol) and $(^tBuN)_2S$ (2.1 g, 12 mmol) were dissolved in heptane (50 mL) under an argon atmosphere and refluxed for 3 h, during which a slow stream of argon was bubbled through the solution. A significant amount of black crystals precipitated. Heptane was evaporated under a reduced pressure, and the residual black precipitate together with a small amount of oily material was dissolved in a minimum amount of benzene. The solution was separated via column chromatography (4 × 20 cm) on alumina (deactivated with 10 wt % of water) into three bands. The first dark brown band was eluted with benzene/dichloromethane (1/1). Evaporation of the solvent and addition of hexane to the residue gave dark crystals and colorless crystals. The colorless crystals, which were characterized by infrared and NMR spectra as $(^tBuNH)_2CO$, were removed by high-vacuum sublimation at 50 °C. The residual dark solid was recrystallized from benzene/hexane to give dark crystals (239 mg) that were identified as a ca. 1/1 mixture of **1** and **2**. The second greenish brown band on the column was eluted with dichloromethane. Addition of hexane to the concentrated (ca. 2 mL) eluent gave dark crystals of $[Co(ZCp)]_3(CO)(S)$ (432 mg, 19% yield), mp 113–115 °C dec. Anal. Calcd for $C_{22}H_{21}Co_3O_7S$: C, 43.6; H, 3.5; S, 5.3. Found: C, 43.6; H, 3.5; S, 5.5. $^1H$ NMR ($CD_2Cl_2$): $\delta$ 3.76 (s, 3 H); $\delta$ 4.72 (t, 2 H, $J$(HH) = 2.2 Hz); $\delta$ 5.21 (t, 2 H, $J$(HH) = 2.3 Hz). Dark crystals of pure **2** were isolated from the mixture with **1** by repeated chromatography and recrystallization (yield 20 mg), mp 103–104 °C dec. Anal. Calcd for $C_{21}H_{21}Co_3O_6S_2$: C, 41.3; H, 3.5; S, 10.5. Found: C, 41.4; H, 3.5; S, 10.4.

**X-ray Crystal Structure Determination of 1.** Crystallographic data are as follows: $C_{25}H_{30}Co_3NO_6S$, $M_r$ = 649.38, triclinic, $a$ = 10.057 (3) Å, $b$ = 14.716 (4) Å, $c$ = 9.680 (3) Å, $\alpha$ = 92.15 (3)°, $\beta$ = 111.48 (2)°, $\gamma$ = 81.34 (3)°, $V$ = 1317.6 (7) Å$^3$, $\lambda$ = 0.71069 Å, space group $P\bar{1}$, $Z$ = 2, $D_{calcd}$ = 1.637 g cm$^{-3}$, $F(000)$ = 664, approximate crystal size 0.21 × 0.61 × 0.84 mm, $\mu$(Mo K$\alpha$) = 19.80 cm$^{-1}$.

X-ray measurements were carried out with a Rigaku four-circle diffractometer equipped with a graphite monochromator. $\omega$-2$\theta$ scans and 10-s stationary background counts were made at the lower and upper limits of each scan. A constant scan speed of 0.06° s$^{-1}$ was used. The data were corrected for Lorentz and polarization effects but not for absorption. A total of 6423 unique reflections in the ranges $\pm h$, $\pm k$, $+l$ and 2.8 ≤ 2$\theta$ ≤ 55.0° were measured, of which 4339 independent reflections having $I \geq 3\sigma(I)$ were used in subsequent analysis.

The structure was solved from direct and Fourier methods and refined by block-diagonal least squares with anisotropic thermal parameters in the last cycles for all non-hydrogen atoms. Hydrogen atoms for the three $C_5H_4CO_2Me$ rings were placed in calculated positions, while those for the methyl groups were located from a difference Fourier map. In the refinements unit weights were applied. The function minimized in the least-squares refinement was $\sum w(|F_o| - |F_c|)^2$. The computational program package used in the analysis was the UNICS III program system.[10] Final $R$ and $R'$ values were 0.046 and 0.048, respectively. The standard deviation of unit weight, $[\sum w(|F_o| - |F_c|)^2/(m-n)]^{1/2}$, where $m$ and $n$ are the number of reflections and refined parameters ($n$ = 542), was 2.1. Anomalous dispersion corrections[11] for Co were included in the refinement. Neutral-atomic scattering factors were taken from ref 12. Final atomic parameters for the non-hydrogen atoms are given in Table III.

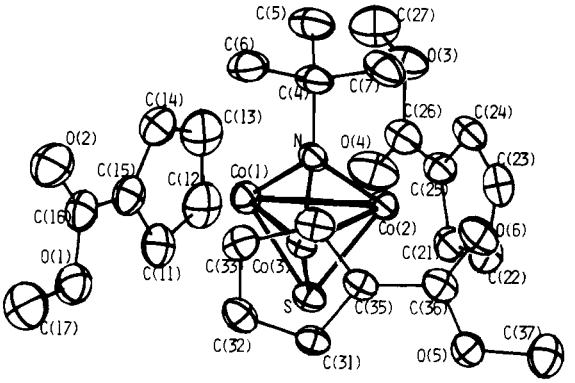


**Figure 1.** Molecular structure of $[Co(C_5H_4CO_2Me)]_3(S)(N^tBu)$ (**1**), showing the atomic numbering scheme.

**Solid-State Magnetic Susceptibility of 1.** The temperature dependence of the magnetic susceptibility of **1** (62.30 mg) was measured under a He atmosphere at 20 kG by means of a vibrating-sample magnetometer (Princeton Applied Research Co., Model 155).

**Molecular Orbital Calculations.** The MO calculations were of the extended Hückel type[13] with a weighted $H_{ij}$ formula.[14] The computational parameters were taken from previous work.[15] The bond lengths and angles for **6** and **7** were based on crystal structures of **1** and **3**.[6a,c] In **5** the Co–Co and N---N distances were assumed to be 2.42 and 2.50 Å, respectively.

## Results and Discussion

**Preparation of $[Co(ZCp)]_3(S)(N^tBu)$ (1, ZCp = $\eta^5$-$C_5H_4CO_2Me$).** In 1968 Otsuka, Nakamura, and Yoshida reported the reaction of $[CoCp(CO)_2]$ with $^tBuN{=}S{=}N^tBu$ to give complexes **3** and $[CoCp]_3(CO)(S)$. The $^tBuN$ fragment in this reaction is trapped by CO, giving urea, $[^tBuNH]_2CO$, and a dimeric complex, $[CoCp]_2[(^tBuN)_2CO]$.[2] Hoping to trap the nitrene fragment as a capping imido ligand, we used CoCp(cod) in place of the CO-containing complex. It gave, however, only trace quantities of a dark green powder that appears to be a dinuclear cobalt complex containing S and $^tBuN$. A clean reaction took place when Co(ZCp)(cod) was used, giving dark brown crystals of **1** as the sole isolable product in 44% yield.

As it was necessary to compare the magnetic behavior of **1** with that of the corresponding trinuclear cobalt complex with two $\mu_3$-S ligands, $[Co(ZCp)]_3(S)_2$ (**2**) was prepared by the Otsuka method.

**Single-Crystal X-ray Analysis of 1.** Black, air-stable single crystals of **1** were grown by the diffusion of hexane into a benzene/ethyl acetate solution at room temperature. Figure 1 shows the perspective view and numbering scheme for the resulting molecular configuration. Selected bond lengths and angles are given in Table I.

The structure may be compared to that of $[CoCp]_3(S)_2$ (**3**), a homologue of **2**, which was reported by Kamijo and Watanabe[6c] and by Frisch and Dahl.[6a] Also of importance are the known structures of the related 48-electron complexes $[CoCp^*]_3(CO)(NH)$,[5] $[CoCp]_3(CO)(S)$,[6a] and $[CoCp]_3(CO)(O)$[1] and the

(8) Hart, W. P.; Rausch, M. D. *J. Am. Chem. Soc.* **1980**, *102*, 1196.
(9) (a) Wakatsuki, Y.; Yamazaki, H. *Bull. Chem. Soc. Jpn.* **1985**, *58*, 2715. (b) Wakatsuki, Y.; Yamazaki, H.; Kobayashi, T.; Sugawara, Y. *Organometallics* **1987**, *6*, 1191.
(10) Sakurai, T.; Kobayashi, K. *Rikagaku Kenkyusho Hokoku* **1979**, *55*, 69.
(11) Cromer, D. T. *Acta Crystallogr.* **1965**, *18*, 17.
(12) *International Tables for X-Ray Crystallography*; Kynoch: Birmingham, England, 1976; Vol. 3, p 13.
(13) Hoffmann, R. *J. Chem. Phys.* **1963**, *39*, 1397. (b) Hoffmann, R.; Lipscomb, W. N. *Ibid.* **1962**, *36*, 2179; *37*, 2872.
(14) Ammeter, J. H.; Bürgi, H.-B.; Thibeault, J. C.; Hoffmann, R. *J. Am. Chem. Soc.* **1978**, *100*, 3686.
(15) Schilling, B. E. R.; Hoffmann, R. *J. Am. Chem. Soc.* **1979**, *101*, 3456.

**Table I.** Selected Bond Distances (Å) and Angles (deg) for **1** with Standard Deviations in Parentheses

| | | | |
|---|---|---|---|
| | Distances | | |
| Co(1)–Co(2) | 2.537 (1) | Co(1)–Co(3) | 2.587 (1) |
| Co(2)–Co(3) | 2.610 (1) | | |
| Co(1)–N | 1.882 (4) | Co(2)–N | 1.866 (4) |
| Co(3)–N | 1.883 (5) | Co(1)–S | 2.159 (2) |
| Co(2)–S | 2.154 (2) | Co(3)–S | 2.153 (2) |
| Co(1)–C(11) | 2.085 (6) | Co(1)–C(12) | 2.119 (8) |
| Co(1)–C(13) | 2.122 (9) | Co(1)–C(14) | 2.111 (6) |
| Co(1)–C(15) | 2.126 (6) | | |
| Co(2)–C(21) | 2.072 (6) | Co(2)–C(22) | 2.091 (6) |
| Co(2)–C(23) | 2.134 (6) | Co(2)–C(24) | 2.131 (6) |
| Co(2)–C(25) | 2.126 (6) | | |
| Co(3)–C(31) | 2.099 (6) | Co(3)–C(32) | 2.123 (6) |
| Co(3)–C(33) | 2.136 (7) | Co(3)–C(34) | 2.116 (6) |
| Co(3)–C(35) | 2.117 (6) | | |
| C(11)–C(12) | 1.424 (11) | C(11)–C(15) | 1.408 (8) |
| C(12)–C(13) | 1.378 (9) | C(13)–C(14) | 1.399 (12) |
| C(14)–C(15) | 1.403 (10) | C(15)–C(16) | 1.462 (10) |
| C(21)–C(22) | 1.396 (10) | C(21)–C(25) | 1.415 (8) |
| C(22)–C(23) | 1.415 (8) | C(23)–C(24) | 1.388 (10) |
| C(24)–C(25) | 1.420 (7) | C(25)–C(26) | 1.460 (9) |
| C(31)–C(32) | 1.401 (8) | C(31)–C(35) | 1.426 (6) |
| C(32)–C(33) | 1.415 (7) | C(33)–C(34) | 1.413 (8) |
| C(34)–C(35) | 1.415 (7) | C(35)–C(36) | 1.455 (8) |
| | Angles | | |
| Co(2)–Co(1)–Co(3) | 61.22 (4) | Co(1)–Co(2)–Co(3) | 60.33 (4) |
| Co(1)–Co(3)–Co(2) | 58.45 (3) | | |
| Co(1)–N–Co(2) | 85.2 (2) | Co(1)–N–Co(3) | 86.8 (2) |
| Co(2)–N–Co(3) | 88.2 (2) | Co(1)–S–Co(2) | 72.07 (5) |
| Co(1)–S–Co(3) | 73.74 (5) | Co(2)–S–Co(3) | 74.60 (5) |
| Co(1)–N–C(4) | 127.7 (4) | Co(2)–N–C(4) | 128.5 (3) |
| Co(3)–N–C(4) | 126.5 (4) | | |

46-electron complex $[CoCp^*]_3(CO)_2$.[7] With the exception of $[CoCp^*]_3(CO)(NH)$, all of these complexes have crystallographic site symmetry $C_{3h}$-3/*m*; therefore, the three Co–Co distances in these complexes are necessarily equal. In the solid state, **1** has no crystallographically imposed symmetry and has three independent Co–Co distances. This is what is expected from removal of the cylindrical symmetry of the cyclopentadienyl ligand by an ester substituent, preventing highly symmetrical crystal packing. In a rougher estimation, however, the three cyclopentadienyl rings with the ester substituent are arranged almost symmetrically around the pseudo $C_3$ axis if one neglects rotation about the C–$CO_2$Me axis containing the ester plane (Figure 1). The bonds between the cyclopentadienyl ring carbon atoms and the ester $\alpha$-carbon lie approximately in the plane of the metal triangle; the deviations of C(16), C(26), and C(36) from the plane defined by Co(1), Co(2), and Co(3) are only −0.081 (7), −0.177 (6), and 0.062 (6) Å. No significant inequality among the three Co–ZCp pairs was found for the bonding of the cyclopentadienyl carbon atoms of a given ring to its cobalt atom.

Deviations of the metal framework from an equilaterial triangle are noteworthy. The difference between the longest Co–Co bond and the shortest one amounts to 0.073 Å (Table I). This marked variation may be caused by two factors: (i) crystal packing forces (in particular the intermolecular S---C(37) and C(7)---C(37) distances of 3.667 (6) and 3.694 (9) Å, respectively, are shorter than the sum of van der Waals radii of S(1.86 Å) and $CH_3$ (2.0 Å)) and (ii) a second-order Jahn–Teller distortion.

The average of the three Co–Co bond lengths in **1**, 2.578 Å, is significantly shorter than that of 2.687 Å in **3**, despite the fact that both are 50-electron triangle clusters. This difference of 0.11 Å in the metal framework has also been noticed during a comparison of the two 48-electron clusters $[CoCp]_3(CO)(O)$ (2.365 (4) Å)[1] and $[CoCp]_3(CO)(S)$ (2.452 (2) Å).[6a] The shorter Co–Co bond in the former complex has been attributed to the smaller triply bridging oxygen ligand,[6a] and the same argument may be applied to the shorter mean Co–Co distance in **1** versus that in **3**. The other factor that controls metal–metal bond lengths may be electronic in origin. Comparison of the Co–Co bond lengths in **1** and $[CoCp]_3(CO)(S)$ (2.452 (2) Å), where both have triply bridging ligands of similar sizes but the former has 50 and the latter 48 electrons, reveals that the metal–metal bond in **1** is 0.13 Å longer. This suggests that the two excess electrons in **1** are in orbital(s) with metal–metal antibonding character.[16]

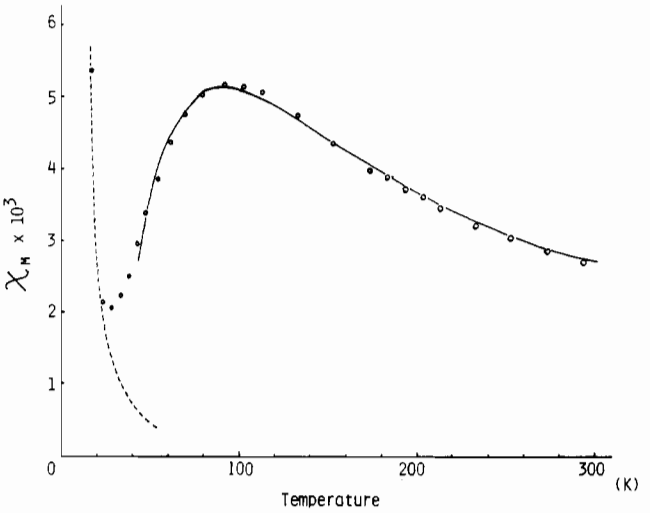


**Figure 2.** Plot of the experimental and calculated (solid line) solid-state magnetic susceptibility of **1** as a function of temperature.

**Solid-State Magnetic Susceptibility of 1.** Figure 2 shows the variation of the molar magnetic susceptibility with temperature for **1**. This curve exhibits a broad maximum at 90 K. Above this critical temperature, the susceptibility, which falls gradually with increasing temperature, approximately obeys the Curie–Weiss law, while below the critical temperature the susceptibility curve falls with the decreasing temperature, rapidly reaching a one-half value at 50 K. The Curie tail (broken line) observed below 30 K is readily attributed to a trace amount of paramagnetic impurity, the effect of which is negligible above 50 K. The magnetic susceptibility of **3** reported by Sorai et al.[17] showed anomalous temperature dependency due to a phase transition at 192.5 K.[17] The 46-electron cluster **4** has been reported to exhibit only a residual magnetic moment, in accordance with its not having two unpaired electrons in the solid state over a similar temperature range.[7] In contrast, the magnetic susceptibility data of **1** fit well to the model where a triplet excited state lies very close to a singlet ground state.

According to Figgis and Martin,[18] the molar susceptibility in such a system can be expressed as

$$\chi_M = \frac{0.25g^2}{T}\left[\frac{1}{1 + (1/3)\exp(J/kT)}\right] + N_\alpha \qquad (1)$$

where $g$ is the spectroscopic splitting factor and is equal to 2 if the magnetic moment arises from spin alone, $k$ is the Boltzmann constant, and $J$ is an energy separation between the singlet and triplet levels. The bracketed term is equal to the mole fraction of the triplet isomer, while $N_\alpha$ represents the temperature-independent magnetism per mole of complex. An excellent least-squares fit of the experimental values to this equation was obtained as shown by the solid line in Figure 2, with the following converged values: $g = 2.19$; $J = 0.286$ kcal/mol (100 cm$^{-1}$); $N_\alpha = 0.95 \times 10^{-4}$.

Extended Hückel MO calculations on a model compound, $[CoCp]_3(S)(NH)$, with idealized $C_{3v}$ symmetry show the presence of a degenerate HOMO (vide infra). Although other vacant orbitals might intervene in the actual complexes, we assume that

(16) The ground-state orbital configuration of **1** under a $C_{3v}$ symmetry is expected to be $e^2a_2^0$ (vide infra). Since the $a_2$ orbital lies very close to the half-filled e orbitals (less than 0.1 eV according to our EXH MO calculations), substantial contribution of the $a_2$ orbital would be expected at room temperature.

(17) Sorai, M.; Suga, H.; Seki, S.; Yoshida, T.; Otsuka, S. *Bull. Chem. Soc. Jpn.* **1971**, *44*, 2364.

(18) Figgis, B. N.; Martin, R. L. *J. Chem. Soc.* **1956**, 3837.

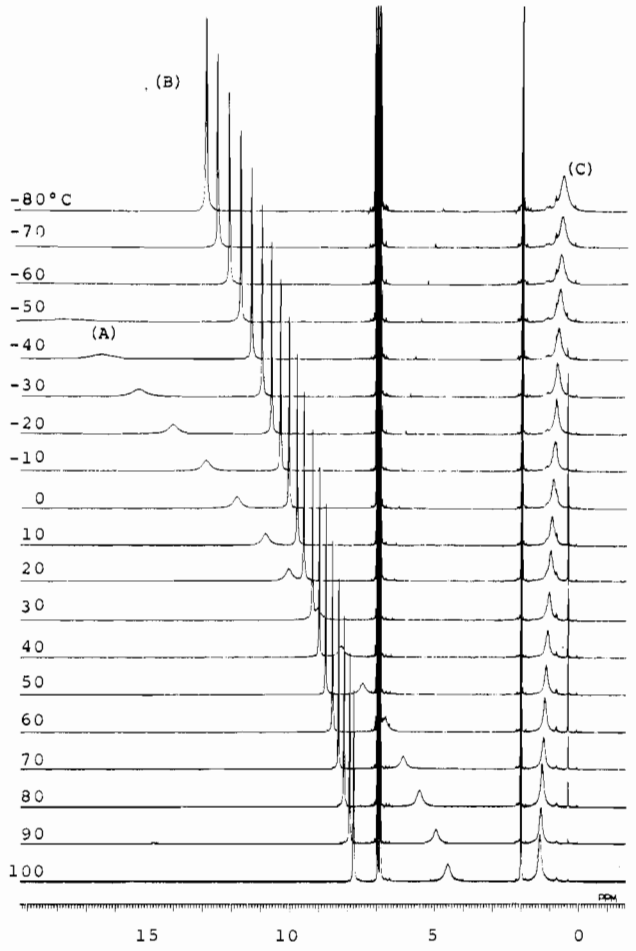


**Figure 3.** Temperature-dependent $^1H$ NMR spectra of [Co($C_5H_4CO_2Me$)]$_3$(S)($N^tBu$) (**1**) in toluene-$d_8$: A, $H_\alpha$ and $H_\beta$ ring protons; B, $CO_2Me$ protons; C, *tert*-butyl protons. The peaks at $\delta$ 2.0 and 7.1 are due to nondeuteriated solvent impurities.

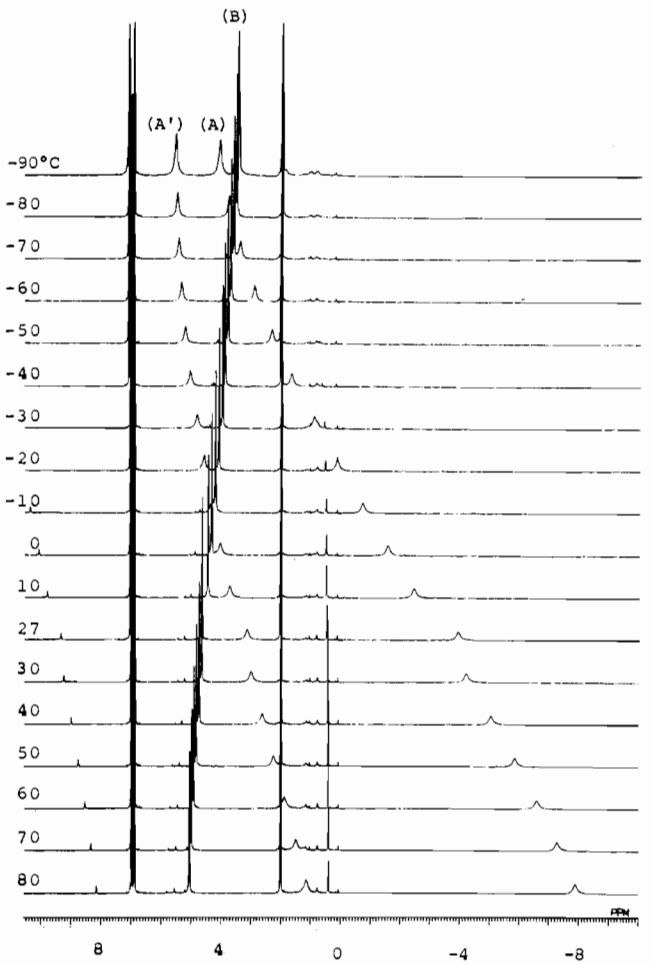


**Figure 4.** Temperature-dependent $^1H$ NMR spectra of [Co($C_5H_4CO_2Me$)]$_3$(S)$_2$ (**2**) in toluene-$d_8$: A and A′, $H_\alpha$ and $H_\beta$ ring protons; B, $CO_2Me$ protons. The peaks at $\delta$ 2.0 and 7.1 are due to nondeuteriated solvent impurities. The sample was contaminated by a trace amount of **1**.

these two orbitals are of primary importance for the determination of the spin state. If the complex is deformed from its assumed 3-fold symmetry and the energy separation between these two orbitals becomes large, the contribution of the singlet state would increase. As we have seen from the resulting X-ray analysis of **1**, deformation of its metal framework from $C_{3v}$ symmetry is relatively large in the solid state, and this must be the main reason for the observed singlet ground state.

**Singlet–Triplet Equilibrium in Solution.** Figure 3 shows the temperature-dependent $^1H$ NMR spectra of **1**. Comparing the spectra with those of **2**, we assign the broad (A) and sharp (B) peaks at low magnetic field to the four cyclopentadienyl protons and the ester methyl protons, respectively, and the broad peak (C) at high magnetic field to the resonance of the $^t$Bu protons. As the temperature is lowered, the resonances for these protons broaden and shift to abnormal values; at high temperatures the resonances are more normal, although those for the methyl protons still deviate largely from a value of ca. $\delta$ 3.55 ppm normally observed for methyl ester protons in diamagnetic complexes.

Variable-temperature $^1H$ NMR spectra of **2** are recorded in Figure 4. Whereas the two expected peaks for two pairs of different cyclopentadienyl protons are not resolved in any spectrum of **1**, in the case of each spectrum of **2**, two such peaks (A and A′) are observed. We tentatively assign peak A to $H_\alpha$ and peak A′ to $H_\beta$. In contrast to the paramagnetic shifts of **1**, those of **2** become smaller as the temperature is lowered, reaching almost zero below 183 K. The parent complex of **2**, [CpCo]$_3$(S)$_2$ (**3**), has been reported to show a similar trend in solution, viz. diamagnetic behavior below 173 K but increasingly paramagnetic with an increase in temperature.[6]

These observations are entirely consistent with the presence of a variable-temperature singlet–triplet spin equilibrium in solution.

**Table II.** Least-Squares Parameters for the Singlet–Triplet Equilibrium of **1** and **2** Obtained from Variable-Temperature $^1H$ NMR Spectra of Each Proton Species

| | peak | assgnt | $\Delta H$, kJ/mol | $\Delta S$, J/(mol·K) | $K'\gamma_0$, Hz·K |
|---|---|---|---|---|---|
| **1** | A | $C_5H_4$ | −24.2 | −81.3 | $1.2 \times 10^6$ |
| | B | $C(O)OCH_3$ | −20.6 | −70.3 | $3.9 \times 10^5$ |
| | C | $t$-$C_4H_9$ | −24.8 | −67.0 | $-7.9 \times 10^4$ |
| | | mean | −23.2 | −72.9 | |
| **2** | A | $C_5H_2$ ($\alpha$) | 18.4 | 58.9 | $-2.9 \times 10^6$ |
| | A′ | $C_5H_2$ ($\beta$) | 17.6 | 47.4 | $-1.8 \times 10^6$ |
| | B | $C(O)OCH_3$ | 21.1 | 73.7 | $3.1 \times 10^5$ |
| | | mean | 19.0 | 60.0 | |

At low temperatures a paramagnetic isomer is the ground state in **1**, while a diamagnetic isomer is the ground state in the case of **2**. A theoretical treatment of the temperature-dependent paramagnetic contact shift of organometallic complexes has been summarized in detail and applied to a closely related tricobalt system by Dahl and co-workers.[7] The paramagnetic frequency shift $\Delta\gamma_i$ (in hertz) is given by

$$\Delta\gamma_i = \frac{K'\gamma_0}{T}\left[\frac{1}{1 + \exp((\Delta H - T\Delta S)/RT)}\right] \qquad (2)$$

where $K' = -A_i(\gamma_e/\gamma_H)(g\beta S(S+1)/6Sk)$ is a constant for a given proton nucleus. Here $A_i$ is the isotropic hyperfine coupling constant for the $i$th proton, $\gamma_e$ and $\gamma_H$ are the magnetogyric ratios of the electron and proton, $g$ is the average spectroscopic splitting factor for the paramagnetic species, and $S$ is the total electron spin. The bracketed term in eq 2, which has been pointed out to be the correct mole fraction of the triplet isomer in solution,

**Table III.** Atomic Coordinates ($\times 10^4$) for **1** with Estimated Standard Deviations in Parentheses

| atom | x | y | z | atom | x | y | z |
|---|---|---|---|---|---|---|---|
| Co(1) | 6595 (1) | 1953 (1) | 6920 (1) | C(14) | 6940 (8) | 559 (4) | 7576 (7) |
| Co(2) | 6705 (1) | 3580 (1) | 7876 (1) | C(15) | 6539 (6) | 611 (4) | 6029 (7) |
| Co(3) | 8173 (1) | 2951 (1) | 6221 (1) | C(16) | 7453 (7) | 218 (4) | 5214 (7) |
| S | 5860 (1) | 3200 (1) | 5580 (1) | C(17) | 7685 (9) | 143 (6) | 2862 (9) |
| O(1) | 6895 (5) | 511 (3) | 3784 (5) | C(21) | 4892 (6) | 4451 (4) | 7901 (6) |
| O(2) | 8550 (5) | −316 (4) | 5714 (6) | C(22) | 5907 (7) | 4980 (4) | 7830 (7) |
| O(3) | 5481 (4) | 2928 (3) | 11052 (4) | C(23) | 7150 (7) | 4793 (4) | 9137 (7) |
| O(4) | 3574 (4) | 3065 (4) | 8928 (5) | C(24) | 6887 (6) | 4151 (4) | 9982 (6) |
| O(5) | 8226 (4) | 5446 (3) | 5480 (4) | C(25) | 5472 (5) | 3931 (4) | 9244 (6) |
| O(6) | 10159 (5) | 5043 (3) | 7533 (5) | C(26) | 4726 (6) | 3282 (4) | 9682 (6) |
| N | 8135 (4) | 2577 (3) | 8044 (4) | C(27) | 4784 (8) | 2330 (6) | 11615 (8) |
| C(4) | 9423 (6) | 2225 (4) | 9397 (5) | C(31) | 8272 (5) | 3631 (4) | 4401 (5) |
| C(5) | 8924 (7) | 1851 (5) | 10547 (7) | C(32) | 8629 (6) | 2684 (4) | 4258 (6) |
| C(6) | 10404 (7) | 1457 (4) | 8982 (7) | C(33) | 9875 (6) | 2358 (4) | 5498 (6) |
| C(7) | 10274 (6) | 3014 (5) | 10059 (7) | C(34) | 10279 (5) | 3124 (4) | 6398 (6) |
| C(11) | 5163 (6) | 1147 (4) | 5480 (7) | C(35) | 9303 (5) | 3921 (4) | 5735 (5) |
| C(12) | 4711 (7) | 1388 (4) | 6695 (8) | C(36) | 9307 (6) | 4835 (4) | 6362 (6) |
| C(13) | 5815 (9) | 1028 (5) | 7966 (8) | C(37) | 8099 (7) | 6362 (4) | 6007 (8) |

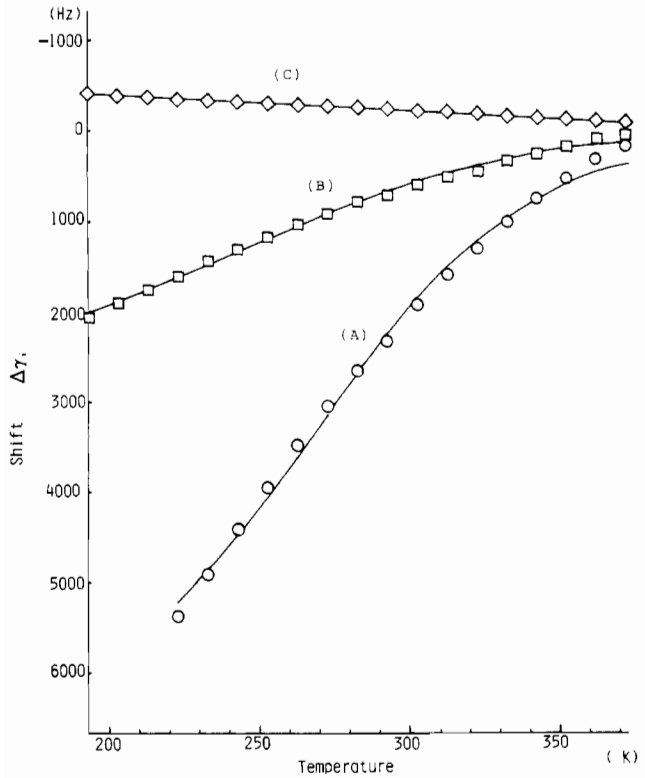


**Figure 5.** Least-squares fit of the temperature-dependent $^1H$ NMR frequency shifts in **1** to eq 2: A, $H_\alpha$ and $H_\beta$ ring protons; B, $CO_2Me$ protons; C, *tert*-butyl protons.

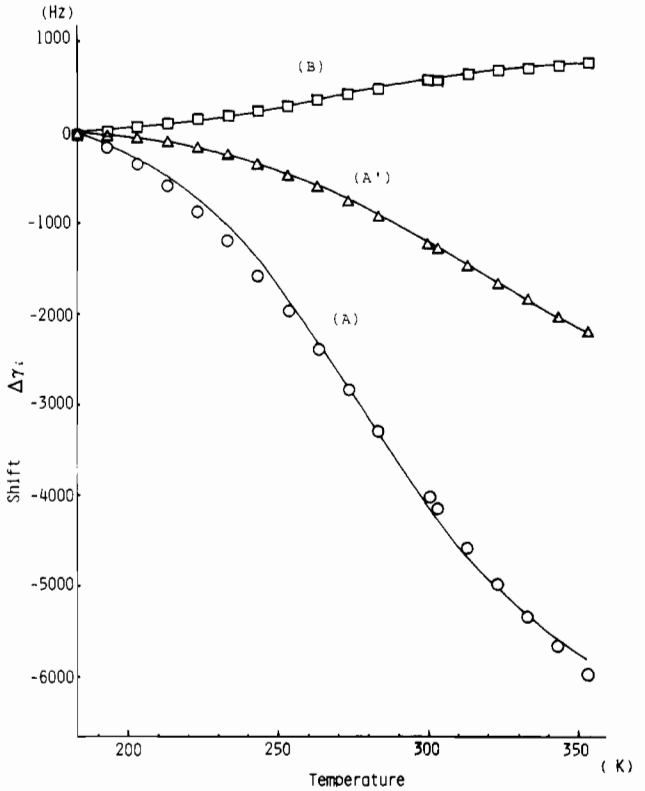


**Figure 6.** Least-squares fit of the $^1H$ NMR frequency shifts in **2** to eq 2: A and A′, $H_\alpha$ and $H_\beta$ ring protons; B, $CO_2Me$ protons.

may be compared to the corresponding term in eq 1. The degeneracy term of $^1/_3$ in eq 1 should be embodied in the entropy change $\Delta S$ in a solution.[19]

Least-squares fits of the paramagnetic shift data to eq 2 are illustrated in Figure 5 for **1** and in Figure 6 for **2**. Table II lists the converged least-squares parameters for each proton species. The negative $\Delta H$ and $\Delta S$ values for complex **1** indicate that the ground state of the complex in solution is a triplet. Conversely, the singlet ground state of **2** is indicated by the positive values of $\Delta H$ and $\Delta S$. With these thermodynamic parameters, at 0 °C for instance, **1** has a triplet ground state with a singlet level ca. 0.8 kcal/mol higher in energy, while **2** has a singlet ground state with a triplet energy level at ca. 0.7 kcal/mol above it.

Extended Hückel MO calculations were carried out on model compounds $[CoCp]_3(NH)_2$ (**5**), $[CoCp]_3(S)(NH)$ (**6**), and $[CoCp]_3(S)_2$ (**7**). Under an assumed $C_{3v}$ symmetry, **6** (and also **5**) was found to have a triplet ground state while **7** had a singlet

**Scheme I.** Schematic Interaction Diagram for $[CoCp]_3$ (Left) and Capping Ligands (Right), Showing the Influence of Metal–Metal Distances on $a_2$ and e MO Energies

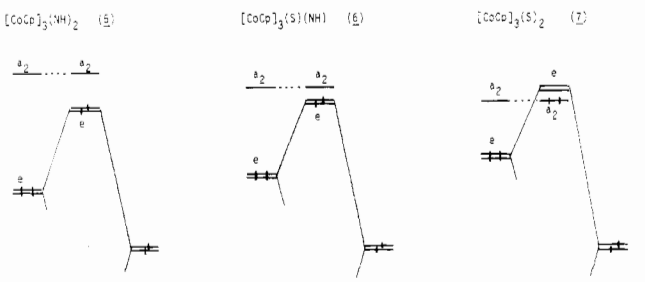


ground state in accordance with the NMR study. The controlling orbitals are the $a_2$ and degenerate e type, whose metal compositions are illustrated in Figure 7. The Cp ligands also contribute to these orbitals significantly; in the case of **6** for instance, the $a_2$ orbital consists of Cp (62%) and Co (38%) contributions and the

(19) Horrocks, W. DeW, Jr. *J. Am. Chem. Soc.* **1965**, *87*, 3779.

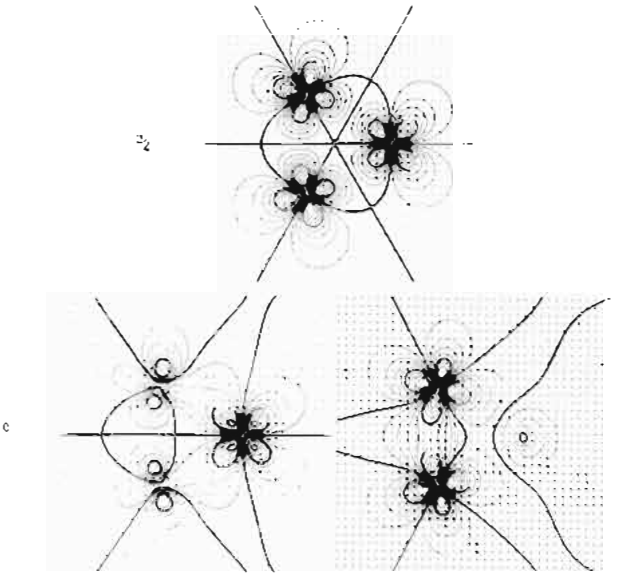

**Figure 7.** Contour diagram, in the triangular metal plane, of the three important $Co_3$ orbitals in $[Co(C_5H_5)]_3(S)(NH)$.

e orbitals consist of Cp (ca. 44%), Co (ca. 42%), and capping ligand (14%) contributions.

Construction of these $a_2$ and e orbitals from the corresponding orbitals of the metal-triangle fragment and a pair of capping ligands is shown in Scheme I. Since the $a_2$ orbital of the metal fragment cannot interact with the orbitals of the capping ligands because of the symmetries, its energy level remains unchanged on construction of the final complex. In contrast, the degenerate e orbitals of the metal fragment interact rather effectively with the $p\pi$ orbitals of the capping ligands, the repulsive part of which gives HOMOs for the total complex in the case of **5** and **6**. In the case of **7**, however, the same interaction results in LUMOs for the total complex since the $a_2$ orbital now lies at lower energy level and takes up the two electrons (Scheme I).

The origin of this different order of the $a_2$ and e orbitals with the change of the capping ligands can be traced back to the different sizes of the triangular metal frames, the largest in **7** and the smallest in **5**, which in turn are governed by sizes of the capping ligands (see the X-ray section). The metal–metal distances used in the present calculations were 2.42 Å for **5**, 2.578 Å for **6**, and 2.688 Å for **7**. In accordance with the orbital character shown in Figure 7, the $a_2$ orbital of the metal fragment stabilizes and the e orbitals slightly destabilize with the increase of the metal–metal distances (Scheme I). Consequently, the energy difference between these two orbital levels of the metal fragment is maximum in **5** and minimum in **7**. In complex **7**, good overlap of the sulfur $3p\pi$ orbitals with the e orbitals of the metal fragment raises these orbitals to the level higher than that of the relatively low-lying $a_2$ orbital.

Although the metal core of **1** in the solid state is frozen in a distorted form by crystal packing forces, it could be relaxed in solution to a configuration close to that of an equilateral metal triangle because its thermodynamically stable isomer in solution at low temperatures is the triplet isomer. As the rotational barrier of a coordinated cyclopentadienyl ring is very small,[20] independent rotational motion of the three ZCp rings in solution would break the 3-fold symmetry only very weakly. On the basis of the MO analysis, the triplet-state orbital configuration of **1** is expected to be $e^2a_2^0$ and that for **2** to be $a_2^1e^1$. The different orbital configuration of the triplet state may be responsible for the different paramagnetic NMR frequency shifts of the ZCp ligands in **1** and **2**; viz., resonances of the ring protons are resolved in **2** but not in **1** and the methyl and ring protons shift in the same direction in **1** but shift in opposite directions in **2**.

**Supplementary Material Available:** Lists of anisotropic thermal parameters for non-hydrogen atoms and positional and isotropic thermal parameters for hydrogens (3 pages); a list of calculated and observed structure factors (19 pages). Ordering information is given on any current masthead page.

(20) Aleksandrov, A.; Struckhov, Yu. T.; Khandkarova, V. S.; Gubin, S. P. *J. Organomet. Chem.* **1970**, *25*, 243.

Contribution from the Department of Chemistry, University of Delaware, Newark, Delaware 19716

# Synthesis and Modes of Coordination of Energetic Nitramine Ligands in Copper(II), Nickel(II), and Palladium(II) Complexes

S. F. Palopoli, S. J. Geib, A. L. Rheingold, and T. B. Brill*

*Received February 3, 1988*

New Cu(II), Ni(II), and Pd(II) complexes of nitraminato ligands derived from methylnitramine, ethylenedinitramine, and a nitroaminotetrazole are reported. A wide variety of modes of metal–ligand coordination have been uncovered by X-ray crystallography. The nitraminato ligands are able to bond through the O or the N donor sites alone or chelate by coordination at both the O and N sites. N,N′-Chelate complexes, bridging nitraminato ligands leading to dimers, and crystalline polymers have also been produced. Crystal data: for *trans*-$[Cu(NH_3)_2\{N(NO_2)CH_3\}_2]$, monoclinic, $P2_1/c$, $a$ = 7.3786 (8) Å, $b$ = 6.2543 (8) Å, $c$ = 10.123 (2) Å, $\beta$ = 102.00 (1)°, $V$ = 457.0 (1) Å$^3$, $Z$ = 2; for $[Cu(en)\{N(NO_2)CH_3\}_2]$, monoclinic, $P2_1/c$, $a$ = 12.282 (3) Å, $b$ = 9.150 (2) Å, $c$ = 10.563 (3) Å, $\beta$ = 113.69 (2)°, $V$ = 1087.0 (6) Å$^3$, $Z$ = 4; for $[Cu(NH_3)_2\{N(NO_2)CH_2CH_2N(NO_2)\}]$, triclinic, $P\bar{1}$, $a$ = 5.851 (2) Å, $b$ = 6.392 (4) Å, $c$ = 6.501 (3) Å, $\alpha$ = 97.24 (4)°, $\beta$ = 108.02 (4)°, $\gamma$ = 111.46 (4)°, $V$ = 207.2 (2) Å$^3$, $Z$ = 1; for $\beta$-$[Ni(H_2O)_4\{N(NO_2)CH_2CH_2N(NO_2)\}]$, monoclinic, $C2/c$, $a$ = 12.584 (3) Å, $b$ = 7.867 (2) Å, $c$ = 10.627 (2) Å, $\beta$ = 111.18 (2)°, $V$ = 980.9 (5) Å$^3$, $Z$ = 4; for $\alpha$-$[Ni(H_2O)_4\{N(NO_2)CH_2CH_2N(NO_2)\}]$, monoclinic, $P2_1/n$, $a$ = 13.508 (2) Å, $b$ = 11.166 (2) Å, $c$ = 14.133 (2) Å, $\beta$ = 114.23 (1)°, $V$ = 1942.3 (5) Å$^3$, $Z$ = 8; for $[Ni(NH_3)_3\overline{NNNNCNNO_2}]_2$, monoclinic, $P2_1/n$, $a$ = 7.200 (1) Å, $b$ = 16.864 (3) Å, $c$ = 7.349 (1) Å, $\beta$ = 114.25 (2)°, $V$ = 813.5 (3) Å$^3$, $Z$ = 2; for $[Cu_2(en)_2\{N(NO_2)CH_2CH_2N(NO_2)\}_2]\cdot 2H_2O$, triclinic, $P\bar{1}$, $a$ = 7.727 (5) Å, $b$ = 10.248 (6) Å, $c$ = 11.367 (7) Å, $\alpha$ = 90.90 (5)°, $\beta$ = 108.26 (5)°, $\gamma$ = 96.82 (5)°, $V$ = 847.4 (9) Å$^3$, $Z$ = 1.

## Introduction

Many organic nitramines are well-known for their exothermic, autocatalytic thermal decomposition. Thus, they are of interest as rocket propellants and explosives. Concern about the amount of stored energy in these molecules may have inhibited investigations of their coordination tendencies despite the fact that selected nitramines would form an interesting class of ligands.[1-3] One unusual feature is that the atom geometry at the amine donor

(1) (a) Franchimont, A. P. N. *Rec. Trav. Chim. Pays-Bas* **1894**, *13*, 307. (b) Davis, T. L.; Ou, C. W. *J. Am. Chem. Soc.* **1934**, *56*, 1064. (c) Liebig, D. M.; Robertson, J. H. *J. Chem. Soc.* **1965**, 5801.

0020-1669/88/1327-2963$01.50/0 